Hydrogen Embrittlement and Fracture Toughness of a Titanium Alloy with Surface Modification by Hard Coatings

S.-C. Lee, W.-Y. Ho, C.-C. Huang, E.I. Meletis, and Y. Liu

The effect of hydrogen embrittlement on the fracture toughness of a titanium alloy with different surface modifications was investigated. Disk-shaped compact-tension specimens were first coated with different hard films and then hydrogen charged by an electrochemical method. Glow discharge optical spectrometry (GDOS), scanning electron microscopy (SEM), and x-ray diffractometry (XRD) were applied to analyze the surface characteristics. The results revealed that fracture toughness of the as-received titanium alloy decreased with the increase of hydrogen charging time. Fracture toughness of the alloy after plasma nitriding or ion implantation, which produced a TiN_x layer, decreased as well, but to a lesser extent after cathodic charging. The best result obtained was for the alloy coated with a CrN film where fracture toughness was sustained even after hydrogen charging for 144 h. Obviously, the CrN film acted as a better barrier to retard hydrogen permeation, but it was at the sacrifice of the CrN film itself.

Keywords

fracture toughness, hydrogen embrittlement, ion implantation, plasma nitriding, titanium alloy

1. Introduction

THE effects of hydrogen on the mechanical properties of titanium alloys are well documented (Ref 1-6). For Ti-6Al-4V alloys, Lucas (Ref 6) showed that the tensile strength and ductility were not affected significantly by hydrogen concentrations up to 200 wt ppm. However, a fracture toughness study using chevron-notched short-bar (CNSB) specimens concluded that fracture toughness exhibited a marked dependence on the hydrogen concentration in titanium alloys (Ref 6). Current methods of alleviating hydrogen attack and hydrogen embrittlement problems were evaluated (Ref 7-10). Surface modification to produce a hydrogen impermeable coating is one of the control techniques for titanium alloys of technical and economic value. Murray (Ref 8) suggested that both metallic and nonmetallic solid films on the substrate can prevent or reduce hydrogen entry if the film possessed less binding energy for hydrogen than the base material, or low solubility and/or low diffusivity for hydrogen.

Plasma nitriding and hard coatings by physical vapor deposition successfully increase surface hardness and wear resistance of titanium alloys (Ref 11-13). Since these methods will alter the surface compositions of the titanium alloys, fracture toughness and susceptibility of hydrogen embrittlement may thus be affected as well when subjected to hydrogen permeation. This research employed three different kinds of surface modification techniques on Ti-6Al-4V in order to evaluate their effects on fracture toughness and the feasibility of preventing hydrogen embrittlement of the material.

S.-C. Lee and **C.-C. Huang,** Dept. of Materials Engineering, Tatung Institute of Technology, Taipei, Taiwan, 10451; **W.-Y. Ho,** Dept. of Mechanical Engineering, Tatung Institute of Technology, Taipei, Taiwan, 10451; and **E.I. Meletis** and **Y. Liu,** Dept. of Mechanical Engineering, Louisiana State University, Baton Rouge, LA 70803, USA.

2. Experimental Procedure

The Ti-6Al-4V alloy used in this study was obtained commercially in a 40 mm diam rod. Table 1 lists the chemical compositions. Specimens from the rod metal were machined into disk-shaped compact tension (CT) specimens, as shown in Fig. 1, according to the specification of ASTM E 399 (Ref 14). Specimens were metallographically polished prior to the test in order to remove the oxide or hydroxide layer on the surface, which might act as barriers to cause poor surface coating or hydrogen uptake.

Three different kinds of surface modification techniques, namely, plasma nitriding, ion implantation processing, and physical vapor deposition (PVD), were executed to coat the specimens. Plasma nitriding was performed by a triode ion nitriding system with standard procedure as in Ref 12. Ion implantation processing was executed in a vacuum chamber at 555 °C. The sputtering gas was a mixture of nitrogen and argon. The plasma current density was 5 mA/cm^2, and the bias energy was 500 eV. Random-arc evaporation PVD was carried out to deposit a CrN coating on the titanium alloys. Before CrN coating, the specimens were plasma etched in the PVD chamber in order to further clean the substrate. During CrN deposition, the substrate temperature was kept at a maximum of 450 °C, and the total gas pressure of the hydrogen and nitrogen gases was maintained at 1 Pa. XRD analyses with CuKα radiation and SEM were applied to characterize the microstructure and the morphologies of the surface layers.

Cathodic charging of hydrogen was carried out by an electrochemical method in 0.1 N HNO_3 solution. The solution contained 1 g/L thiourea as a hydrogen recombination poison. The coated specimens were masked with acid-resistant tape to ex-

Table 1 Composition of Ti-6Al-4V alloy

Composition, wt%						
Ti	Al	V	Fe	C	O	H
Balance	6.224	4.314	0.228	0.029	0.303	0.004

pose a hydrogen charging area, as depicted in Fig. 1. Cathodic charging was for 48, 96, or 144 h at 30 °C. Current density was maintained at a constant value of 10 mA/cm^2. Fracture toughness testing was conducted immediately after the cathodic charging.

A plane stress fracture toughness (K_c) test was executed according to ASTM E 561 (Ref 15) to evaluate the fracture toughness of the specimens. The CT specimens were tested by a 25-ton MTS (Materials Testing System, USA) hydro-servo dynamic testing machine at ambient temperature. All specimens were fatigue precracked to a crack length within 0.45 to 0.55 W. (W is shown in Fig. 1.) After cathodic charging, the precracked specimens were subjected to preliminary fatigue crack growth before final fracturing to eliminate the blunting effect of the crack tip during chemical permeation of hydrogen into the specimen subsurface. The plane stress fracture toughness (K_c) data were calculated (Ref 15):

$$K_c = \frac{P}{B\sqrt{W}} \times f\left(\frac{a}{W}\right)$$

where P is applied load, B is specimen thickness, and W is total specimen width measured from the load line. Also,

$$f(a/W) = \left[\left(2+\frac{a}{W}\right)/\left(1-\frac{a}{W}\right)^{3/2}\right]\left[0.886 + 4.64\left(\frac{a}{W}\right) - 13.32\left(\frac{a}{W}\right)^2 + 14.72\left(\frac{a}{W}\right)^3 - 5.6\left(\frac{a}{W}\right)^4\right]$$

is valid for any $a/W \geq 0.35$. a is a_e, the effective half crack size, that is, the total physical crack length, a_p, plus plastic zone adjustment, r_y. r_y is $(1/2\pi)(K_c^2/\sigma_y^2)$ where σ_y is 0.2% offset yield strength of the material.

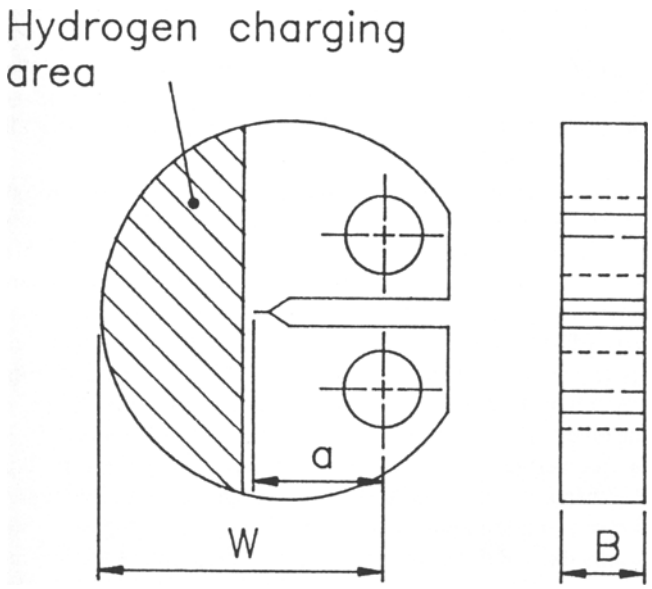

Fig. 1 Dimensions of disk-shaped compact tension specimen. w = 30 mm, B = 5 mm, and a = 13.5 to 16.5 mm

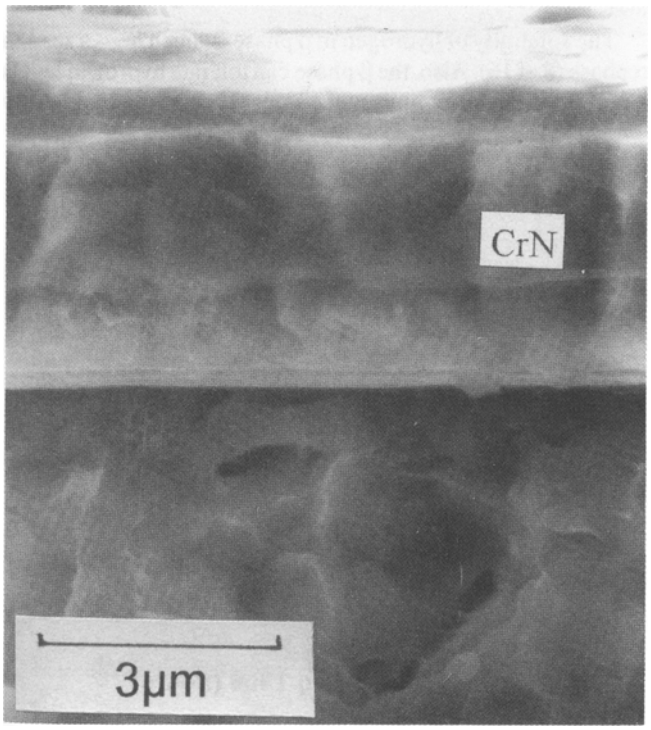

Fig. 2 Cross-sectional view of CrN film on Ti-6Al-4V alloy

3. Results and Discussion

3.1. *Effect of Hydrogen Charging Time on Fracture Toughness*

The effect of different cathodic charging times on the K_c of specimens was determined on the as-received Ti-6Al-4V alloys

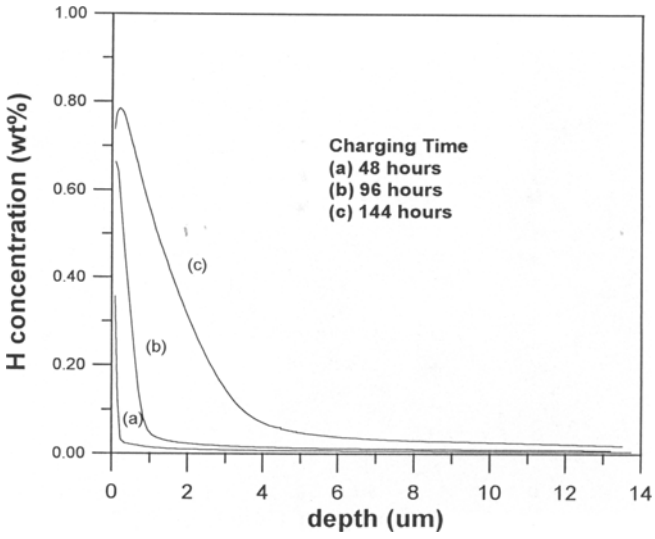

Fig. 3 Hydrogen concentration profiles of as-received Ti-6Al-4V alloy with different hydrogen charging times

with or without CrN coatings. The CrN film on the titanium alloy is shown in Fig. 2. The film thickness was measured to be near 3.5 μm. Hydrogen permeation into the as-received specimens after cathodic charging for different time periods was analyzed by a glow discharge optical spectrometer (GDOS).

Results of hydrogen concentration profiles of the bulk materials are depicted in Fig. 3. The hydrogen concentration increases with increase of charging time. Since hydrogen permeability is a product of diffusivity and solubility of charged materials (Ref 2), longer charging time results in higher hydrogen concentrations in the bulk material for the as-received titanium alloy.

The fracture toughness of tested specimens with and without CrN coating are shown in Fig. 4. The K_c of the as-received alloys decreased with the increase of cathodic charging times. For the specimen charged to 144 h, the K_c value dropped significantly from 101 to 83 MPa$\sqrt{m}$. With the CrN coating, the fracture toughness of as-deposited specimens decreased to 93 MPa$\sqrt{m}$ as compared to that of as-received specimens. However, the CrN film coating obviously provided protection from hydrogen attack so that the K_c data remained virtually unchanged even though the specimens were hydrogen charged for 144 h.

According to ASTM E 561 specifications, the K_c of a CT specimen is affected by the presence of the plastic deformation at the crack tip, which acts as though the crack is slightly longer than actual. A calculated value of crack-tip plastic-zone adjustment (r_y) is thus added to the actual crack length (a_p).

Figure 5 depicted the r_y of fracture CT specimens after cathodic charging for different time periods. Similar results were observed on r_y as on the K_c for specimens with and without CrN coating. In addition, for the specimen without cathodic charging, CrN coating with higher hardness resulted in less r_y, which was attributed to the coating acting as a constraint to retard the plastic deformation of crack tip. Therefore, the calculated r_y values were decreased so that the K_c of the specimen with a CrN coating also decreased because of the reduced effective crack length (a_e). The decrease of fracture toughness and decrease in crack-tip plastic region of the as-received titanium alloy is a consequence of the hydrogen absorption into the bulk material. On the other hand, the CrN-coating might have provided hydrogen permeation shielding.

An examination of the fracture surface of specimens with or without CrN coating, for the as-received specimens, showed that shear lips caused by the crack-tip plastic deformation were quite obvious on the entire fracture surface. After 144 h of cathodic charging, such shear lips virtually disappeared. Quantitatively, the decrease of r_y revealed this brittle fracture transition of titanium alloys induced by high hydrogen absorption. Contrary to the as-received specimen, for the CrN-coated titanium alloy, even the specimen that has been cathodically charged for 144 h, the shear lips were quite pronounced on all of the fractured surfaces.

Examination of the microstructures of the titanium alloys with or without CrN coating was carried out on the specimens with or without cathodic charging to 144 h, as shown in Fig. 6(a to d). The uncharged, as-received specimen (Fig. 6a) was characterized by equiaxed grains of α (light) and continuous β matrix (dark) containing platelet α. After the as-received specimen was charged for 144 h, the β phase changed from continuous to discontinuous matrix, as shown in Fig. 6(b). On the other hand, specimens with Cr-N coating still retained similar microstructures to that of the as-received alloy (Fig. 6c). For the charged CrN-coated specimen, change of microstructure of β phase to discontinuous matrix is also shown in Fig. 6(d), but it only existed in the area near the surface. Figure 6(d) also revealed the disappearance of CrN film after hydrogen charging for 144 h. This implied that although CrN film acted as a barrier to retard hydrogen permeation into the substrate, the CrN film itself was sacrificed during long-term charging in HNO_3 solution.

The solubility of hydrogen in β phase is much higher than in α phase (Ref 16). Also, the β phase can tolerate hydrogen levels close to its solubility limit without significant loss in ductility

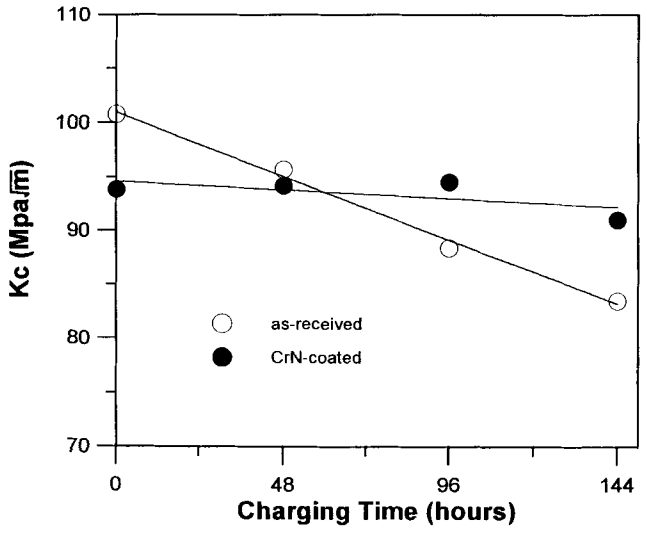

Fig. 4 Fracture toughness of Ti-6Al-4V alloy with different hydrogen charging times

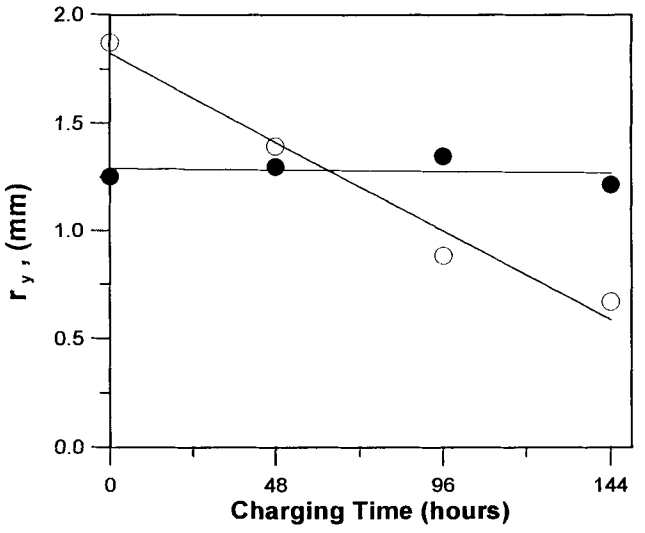

Fig. 5 Calculated crack-tip plastic deformation radius, r_y, of Ti-6Al-4V alloy with different hydrogen charging time

or the onset of stress-induced hydride formation. Hack and Leverant (Ref 17) stated that for α/β titanium alloys, a continuous layer of β phase, which surrounds an α platelet, can act as a crack blunter if the α were to cleave. However, the discontinuous β phase will not present an effective barrier to cleavage. On the other hand, for the as-received specimen, the depth of the

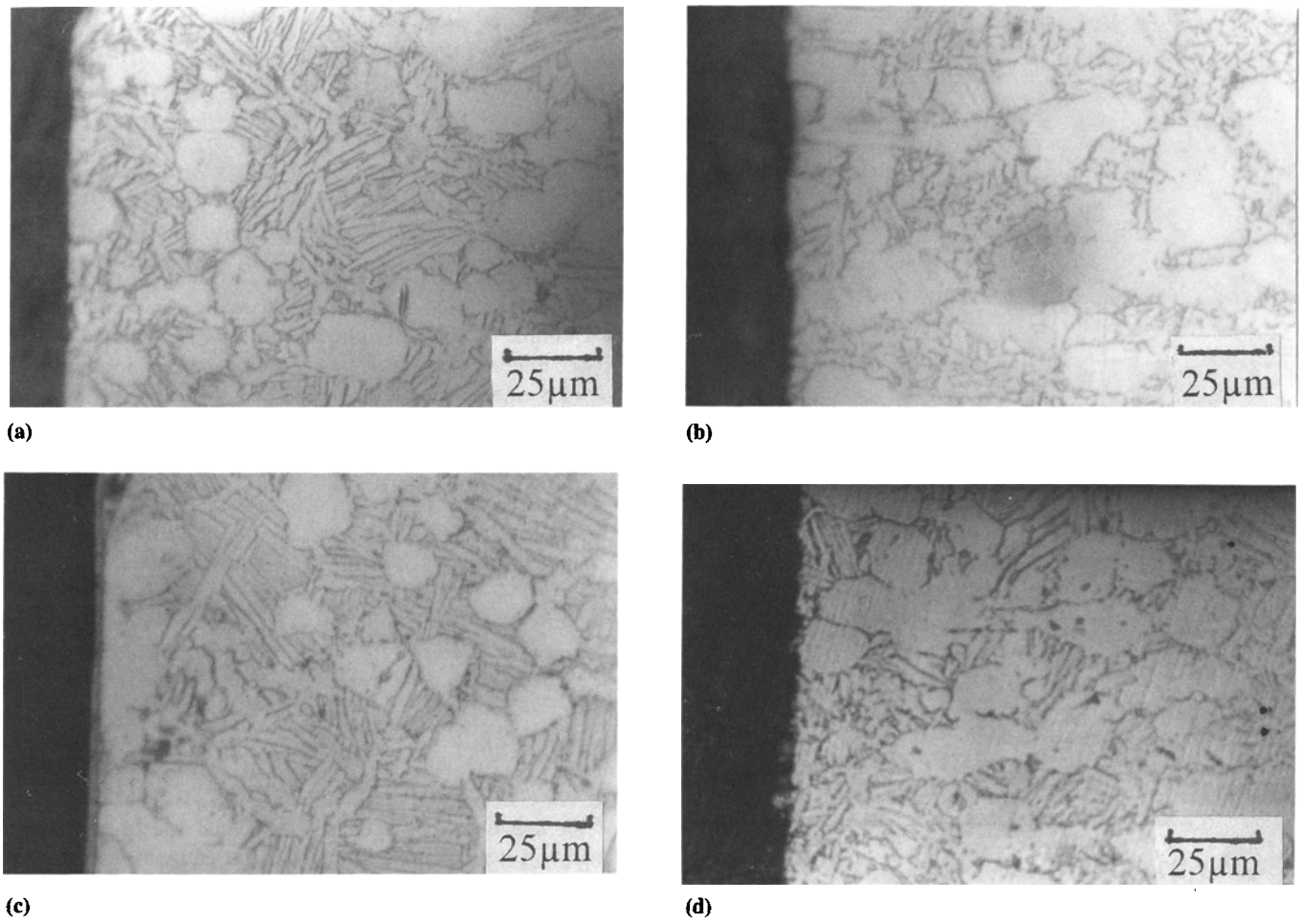

(a) (b) (c) (d)

Fig. 6 Microstructure of specimen charged for 144 h. As-received specimen: (a) uncharged area, (b) charged area. CrN-coated specimen: (c) uncharged area, (d) charged area

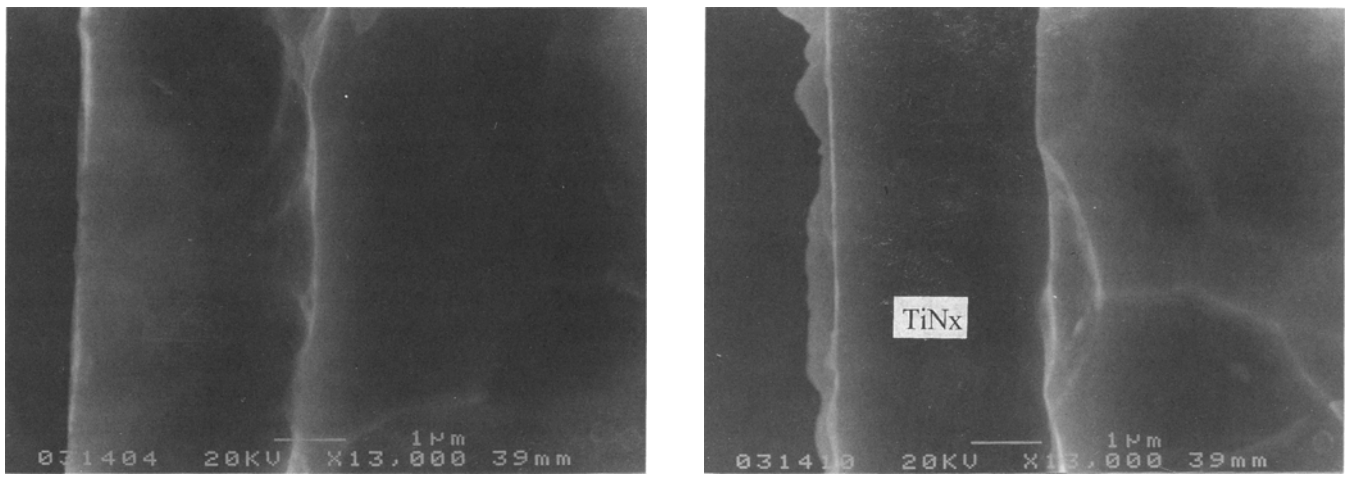

(a) (b)

Fig. 7 Cross-sectional view of TiN layers on the Ti-6Al-4V alloy. (a) Plasma ion nitriding. (b) Ion implantation

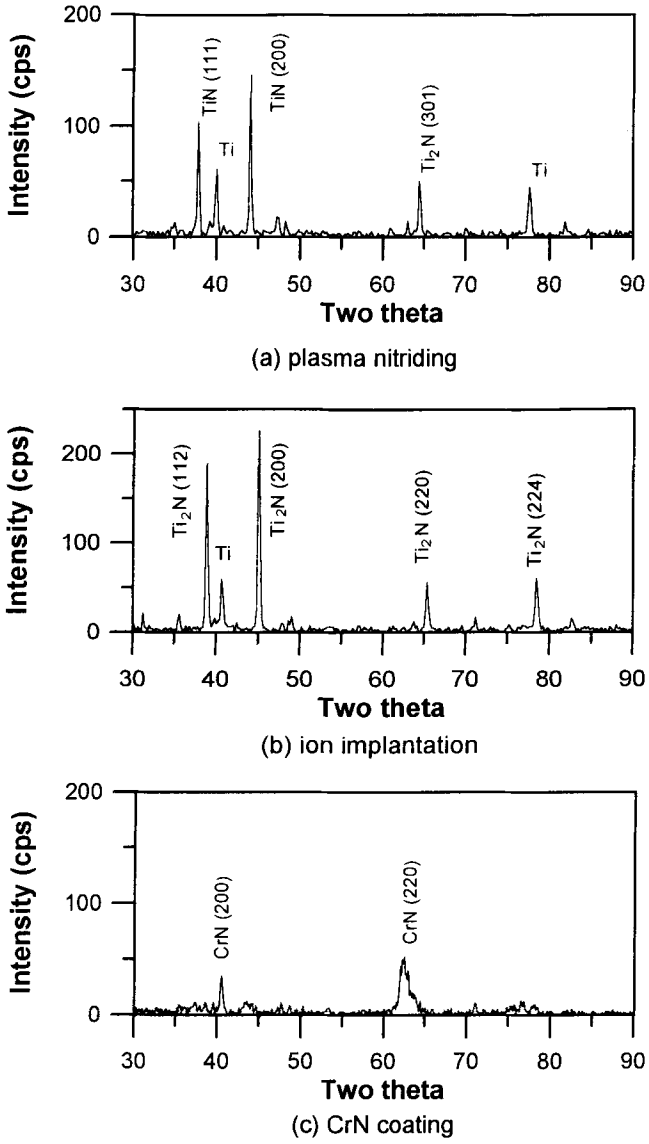

Fig. 8 XRD patterns of specimens with different surface treatments

zone where β phase changed from a continuous to a discontinuous texture after being charged for 144 h was near 500 μm. Therefore, with respect to the specimen thickness, the depth of the total texture changed zone on both sides of the charged specimen was roughly near 1/5. This value correlated closely to the ratio of fracture toughness decrease for the as-received specimen with cathodic charging for 144 h. Thus, the decrease of fracture toughness for the as-received specimen subjected to hydrogen charging was caused by the change of β phase from continuous to discontinuous morphology, which in turn eliminated its ability to blunt crack during fracture.

As a conclusion, fracture toughness of the as-received Ti-6Al-4V alloy was apparently influenced by the high hydrogen permeation into the substrate after cathodic charging. With a CrN thin film, it effectively acted as a barrier to significantly retard the permeation of hydrogen into the material and thus preserve the fracture toughness of the material.

Table 2 Fracture toughness of specimens with different surface treatments

Surface treatment	Surface layer	Uncharged		Charged to 144 h	
		K_c, MPa$\sqrt{m}$	r_y, mm	K_c, MPa$\sqrt{m}$	r_y, mm
As-received	...	100.78	1.873	83.49	0.670
Plasma nitrided	TiN, Ti_2N	89.33	1.498	80.75	1.026
Ion implantation	Ti_2N	98.00	1.472	90.88	0.767
CrN coated	CrN	93.83	1.254	91.03	1.215

3.2 *Effect of Different Hard Coating on Fracture Toughness*

Different surface treatments were evaluated to determine the effect of hydrogen embrittlement on the fracture toughness of a sample cathodically charged for 144 h. Specimens with TiN coating treated by plasma nitriding and ion implantation were tested to compare them with the CrN-coated specimen. The thickness of the TiN_x layers for these treated specimens was measured at approximately 3.2 μm, which was similar to the thickness of the CrN coating, as shown in Fig. 7.

Figure 8 shows the XRD analysis of specimens with different surface coatings. The plasma-nitrided specimen showed the presence of compound layers of δTiN and εTi_2N phases on the surface (Fig. 8a). The diffraction patterns of specimens with ion implantation treatment detected only εTi_2N phases on the surface, as shown in Fig. 8(b). As for the CrN-coated specimens, diffraction patterns revealed the CrN phase with strong (200) and (220) preferred orientation (Fig. 8c).

Results of fracture toughness for specimens with different surface treatment are shown in Table 2. An appreciable hydrogen effect in decreasing fracture toughness was observed on all of the specimens except the CrN-coated specimen. For the specimen with plasma ion nitriding treatment, the fracture toughness reduced by nearly 10% after being cathodically charged for 144 h. Similarly, a 7% decrease of fracture toughness was observed for the ion implanted specimen after cathodic charging. Both plasma ion nitrided and ion-implanted specimens exhibited the decrease of fracture toughness to some extent, but the decrease was less than that of the hydrogen-charged as-received specimen. The surface compound layers of δTiN and εTi_2N phases also may have retarded the hydrogen permeation into the substrate. However, the compound layer was sacrificed during hydrogen charging in 144 h time. Thus, the hydrogen permeated into the substrate when the layer disappeared. But the CrN-coated specimen almost retained its fracture toughness as compared to the as-deposited specimen after being charged for 144 h. Thus, the CrN film acted as a better barrier than TiN layers to protect the bulk material from the corrosion of HNO_3 solution and hydrogen permeation into the substrate during long-term charging.

Figures 9(a to d) show SEM photomicrographs of the specimen fracture surface after being charged for 144 h. Clearly, the fracture surface morphologies were virtually indistinguishable, except for the as-received specimen. The as-received specimens that were cathodically charged for 144 h showed the formation of subsurface cleavage facets, which was associated with hydrogen embrittlement (Fig. 9a).

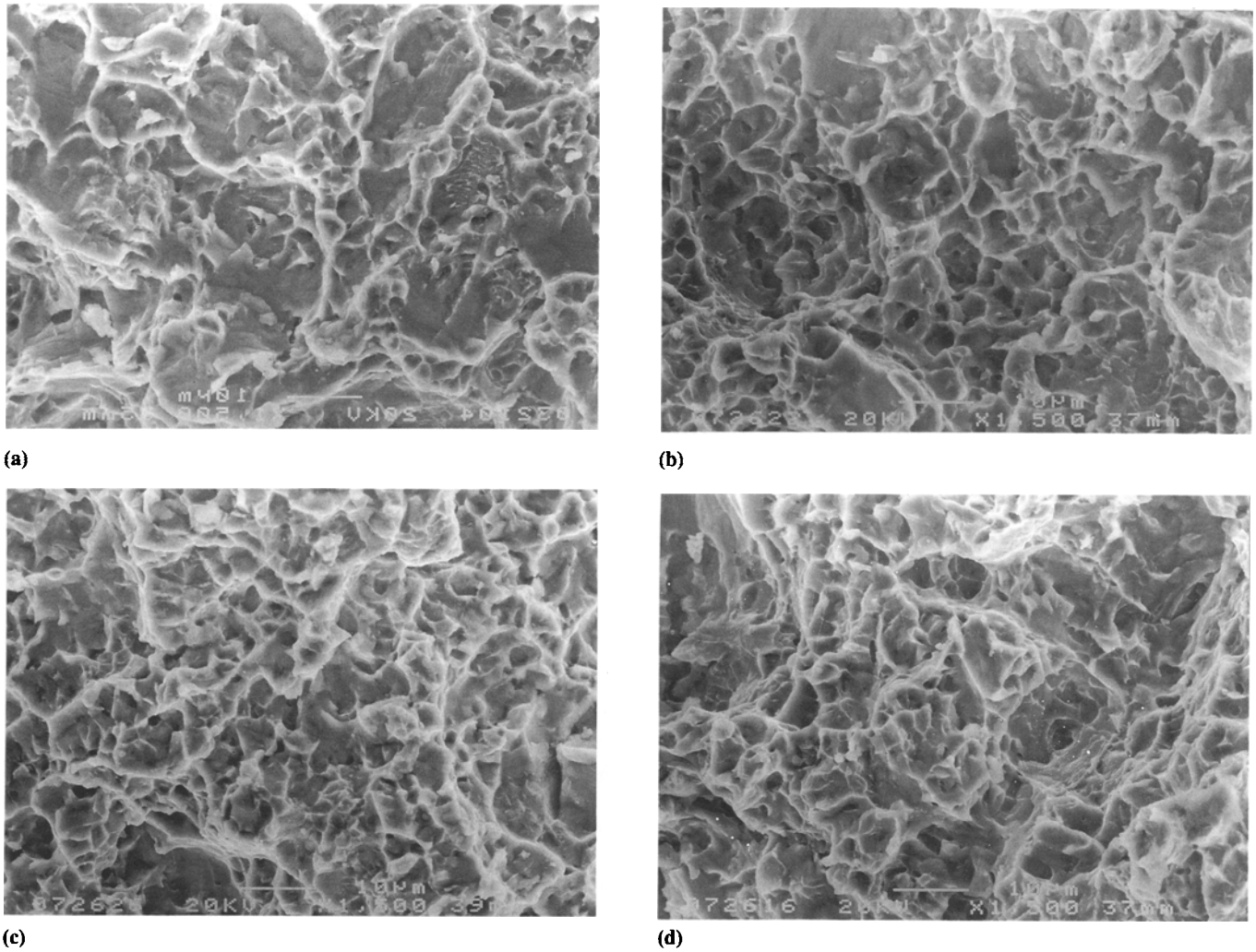

(a) (b) (c) (d)

Fig. 9 SEM morphologies of fracture surface for specimens hydrogen charged to 144 h. (a) As-received. (b) Plasma nitriding. (c) Ion implantation. (d) CrN coating.

4. Conclusions

- The fracture toughness of the as-received Ti-6Al-4V alloy decreased with the increase of hydrogen charging time. The decrease of the fracture toughness in the as-received titanium alloy was caused by the change of β phase from continuous to discontinuous structure, which allowed fracturing to occur through hydrogen embrittlement.
- Fracture toughness of the alloy after plasma nitriding or ion implantation (TiN_x layer of 3.2 μm) decreased as well after cathodic charging to 144 h.
- For the titanium alloy coated with CrN film (about 3.5 μm), fracture toughness remained nearly constant even after hydrogen charging for 144 h. Obviously, the CrN film coated by the arc evaporation PVD process acted as a better barrier to retard hydrogen permeation, but the CrN film itself was also sacrificed during cathodic charging.

Acknowledgments

The authors are grateful for the financial support of this research by the National Science Council, Republic of China, under contract No. NSC83-0405-E036-004.

References

1. D.A. Meyn, Effect of Hydrogen on Fracture and Inert-Environment Sustained Load Cracking Resistance of α-β Titanium Alloys, *Metall. Trans.*, Vol 5, 1974, p 2405-2414
2. S.N. Sankaran, R.K. Herrmann, R.A. Outlaw, and R.K. Clark, Barrier-Layer Formation and Its Control during Hydrogen Permeation through Ti-24Al-11Nb Alloy, *Metall. Trans. A*, Vol 25, 1994, p 89-97
3. S.C. Lee, W.Y. Yo, and T.M Chen, Prevention of Hydrogen Degradation in Titanium by Deposition of TiN Thin Film, *J. Mater. Eng. Perform.*, Vol 3 (No. 6), 1994, p 740-743
4. G.A. Lenning, C.M. Craighead, and R.I. Jaffee, Constitution and Mechanical Properties of Titanium-Hydrogen Alloys, *Hydrogen Damage*, C.D. Beachem, Ed., American Society for Metals, 1979, p 100-109
5. G.Y. Gao and S.C. Dexter, Effect of Hydrogen on Creep Behavior of Ti-6Al-4V Alloy at Room Temperature, *Metall. Trans. A*, Vol 18, 1987, p 1125-1130
6. J.P. Lucas, Hydrogen Effects on Fracture Toughness of Ti-6Al-4V Determined by a Steadily Growing Stable Crack, *Hydrogen Effects on Material*, N.R. Moody and A.W. Thompson, Ed., TMS/AIME, 1990, p 871-880
7. J.P. Hirth and H.H. Johnson, Hydrogen Problems in Energy Related Technology, *Corrosion-NACE*, Vol 32 (No. 1), 1976, p 3-15

8. G.T. Murray, Prevention of Hydrogen Embrittlement by Surface Films, *Hydrogen Embrittlement,* L. Raymond, Ed., ASTM, 1988, p 304-317
9. J.M. Chen and J.K. Wu, Diffusion through Copper-Plated AISI 4140 Steels, *Corros. Sci.,* Vol 33, 1992, p 657-666
10. P. Bruzzoni and R. Garavaglia, Anodic Iron Oxide Films and Their Effect on the Hydrogen Permeation through Steel, *Corros. Sci.,* Vol 33, 1992, p 1797-1807
11. K.T. Kembaiyan, R.D. Doherty, R.P. Singh, and R. Verma, Ion Nitriding of Titanium and Ti-6Al-4V Alloy, *Ion Nitriding and Ion Carburizing,* T. Spalvins and W.L. Kovacs, Ed., ASM International, 1990, p 119-129
12. T.M. Muraleedharan and E.I. Meletis, Surface Modification of Pure Titanium and Ti-6Al-4V by Intensified Plasma Ion Nitriding, *Thin Solid Films,* Vol 221, 1992, p 104-113
13. A. Chen, J. Blanchard, S.H. Han, J.R. Conrad, R.A. Dodd, P. Fetherston, and F.J. Worzala, A Study of Nitrogen Ion-Implanted Ti-6Al-4V ELI by Plasma Source Ion Implantation at High Temperature, *J. Mater. Eng. Perform.,* Vol 1 (No. 6), 1992, p 845-847
14. "Standard Test Method for Plane-Strain Fracture Toughness of Metallic Materials," ASTM E 399-90
15. "Standard Practice for R-Curve Determination," ASTM E 561-92a
16. D.N. Williams, The Hydrogen Embrittlement of Titanium Alloy, *Hydrogen Damage,* C.D. Beachem, Ed., American Society for Metals, 1979, p 185-190
17. J.E. Hack and G.R. Leverant, The Influence of Microstructure on the Susceptibility of Titanium Alloys to Internal Hydrogen Environment, *Metall. Trans. A,* Vol 13, 1982, p 1729-1738